International Journal of Mass Spectrometry 298 (2010) 10–16

Contents lists available at ScienceDirect

International Journal of Mass Spectrometry

journal homepage: www.elsevier.com/locate/ijms

A method for direct measurement of ion mobilities using a travelling wave ion guide☆

Kevin Giles*, Jason L. Wildgoose, David J. Langridge, Iain Campuzano

Waters Corporation, Floats Road, Wythenshawe, Manchester, M23 9LZ, UK

ARTICLE INFO

Article history:
Received 15 January 2009
Received in revised form 2 October 2009
Accepted 12 October 2009
Available online 22 October 2009

Keywords:
Ion mobility
Collision cross-section
Travelling wave
Stacked-ring ion guide

ABSTRACT

The relatively recent introduction of a commercial ion mobility-mass spectrometry instrument has provided access to ion mobility for many investigators for the first time. The mechanism of mobility separation in this instrument differs from classical drift tubes in that travelling voltage waves are used, which has necessitated calibration of the device when collision cross-section (CCS) data are required. Here we present a study into a mode of operation of the travelling wave mobility separator which enables direct determination of mobility and hence CCS values. It is shown that for fixed travelling wave pulse amplitudes and velocities, a minimum mobility is required for an ion species to fully surf on a single wave through the mobility device. For a species with the minimum mobility, the trajectory on the travelling wave front is unique and reproducible. SIMION modelling shows the electric potential profile of the travelling wave to be approximately Gaussian and this is used to establish the field experienced by an ion species on the wave front, ultimately allowing determination of mobility values. With the travelling wave mobility device operating with Helium at 2.5 mbar and equivalent wave velocities of 200–300 m/s, wave amplitudes between 7.9 and 16.2 V were required to establish the mobilities of various singly and multiply charged species ranging in CCS from 147 to 3815 Å^2. We show that using this method, CCS values can be obtained which are within 5% of the results obtained using drift tubes.

1. Introduction

The resurgence of interest in ion mobility spectrometry over the past 10 years has been as a result of a departure from the more traditional use of the technique as a point detector for chemical warfare agents, explosives and illegal drugs [1] into a research tool for investigating species of biological significance and/or for use in the rapid separation of complex mixtures [2–5]. More specifically the development of sophisticated ion mobility-mass spectrometry (IM-MS) systems have raised the profile of the technique such that many more analysts are now considering the potential benefits for their area of work. Perhaps the most significant instrumental developments have been those which have addressed the low transmission efficiency associated with classical drift tube ion mobility spectrometers, particularly when operating at sub-ambient pressure. Notably, radial ion diffusion losses have been minimised through use of periodic focussing ion guides [6], radial ion confinement using radio frequency (RF) ion guides [7–9] and re-focussing of diffuse ion clouds using funnel ion guides [10,11]. Also, the low duty cycle of standard drift tubes has been addressed through use of ion accumulation prior to mobility separation [8,10–14], and through use of discontinuous ion sources such as MALDI [6,15–17]. As a consequence of some of these advances in performance, the ion mobility separator no longer compromises the sensitivity of the mass spectrometer allowing sample analysis at analytically and biologically significant levels.

In more recent years, the introduction of a commercial IM-MS instrument, the Synapt HDMS system from Waters [18], has opened up the area of IM-MS to many more analysts and researchers alike. The Synapt encompasses the benefits of a high transmission mobility separation system, but uses a novel travelling wave (T-Wave) [18,19] device to perform the mobility separation. Whilst the Synapt was developed primarily for the benefits mobility could offer in enhancing the mass spectrometer performance, researchers have also been interested in obtaining ion mobility data to allow determination of structural information on the ion species being investigated. This requires experimental determination of collision cross-section (CCS or Ω) values for the ion species which can be compared with values from computational models to elucidate structure. Ion mobilities and consequently CCS values are directly obtainable from classical, uniform electric field, drift tube IM separators through the expressions [20,21]:

☆ This article is part of a Special Issue on Ion Mobility.

* Corresponding author. Tel.: +44 161 946 2470; fax: +44 161 946 2480.
E-mail address: kevin_giles@waters.com (K. Giles).

1387-3806/$ – see front matter © 2009 Elsevier B.V. All rights reserved.
doi:10.1016/j.ijms.2009.10.008

$$v = KE \quad (1)$$

and

$$\Omega = \frac{3ze}{16N}\left[\frac{2\pi}{\mu k_b T}\right]^{1/2}\frac{1}{K} \quad (2)$$

where v is the drift velocity of an ion of mobility K under the influence of an electric field E, and e is the unit electronic charge, z the number of charges on the ion, N the neutral gas number density, k_b is Boltzmann's constant, T is the neutral gas temperature and μ is the reduced mass of the ion and neutral, given by $(m_i m_n/(m_i + m_n))$, where m_i and m_n are the ion and neutral masses respectively (all values are in SI units). The T-Wave-based mobility separation used in the Synapt instrument is more complex since the electric field is neither uniform nor time independent. Whilst recent work has begun to provide an analytical framework for understanding the mobility separation afforded by the T-Wave device [22] there is currently no 'first principles' approach to deriving mobilities (and hence CCS values) from the experimentally measured ion drift times and the physical parameters of the experimental arrangement. However, a growing number of studies illustrate that the mobility separation afforded by the T-Wave device can be effectively calibrated using species of known CCS derived from drift tube studies [23–31].

Here we report on methodology which facilitates direct determination of ion mobility values using the T-Wave mobility separator [26]. The theoretical concept behind this approach is outlined below.

2. Theory

The geometry and operation of the T-Wave mobility separation device has been described in detail elsewhere [18,19] and will be described only briefly here. In essence, the device consists of a stacked-ring ion guide (SRIG) which is shown schematically in Fig. 1(a). Opposite phases of an RF voltage are applied to adjacent ring electrodes to provide radial ion confinement which results in high transmission efficiency. To propel ions through the device when it is gas-filled a repeating pattern of voltage pulses is used. The pulsed voltage is superimposed on the RF voltage applied to an adjacent pair of electrodes and, after a fixed pulse dwell time, the voltage is stepped to the next electrode pair and so on through the device creating a travelling wave (see Fig. 1(b)). Ion species in the cell will experience the field of an approaching wave and start to drift through the gas accordingly. Ion species above a certain mobility threshold will effectively surf on a single wave through the device and no relative mobility information can be gained. However, ion species below that mobility threshold can be overtaken by the waves and experience both the forward and reverse fields of the pulse. Because the pulse progresses in a forward direction, the ion species spend more time on the forward field than the reverse and, consequently, are still propelled in a forward direction through the device. Mobility separation occurs as a result of lower mobility species being overtaken by the waves more often than higher mobility species and hence taking longer to transit the device. The motion of two ion species, of different mobility, in a T-Wave mobility device has been modelled using SIMION [32] and the results are shown in Fig. 2. In the SIMION model, interaction of the ion species with the background gas was implemented through a user program as a continuous drag force [33]. To simplify

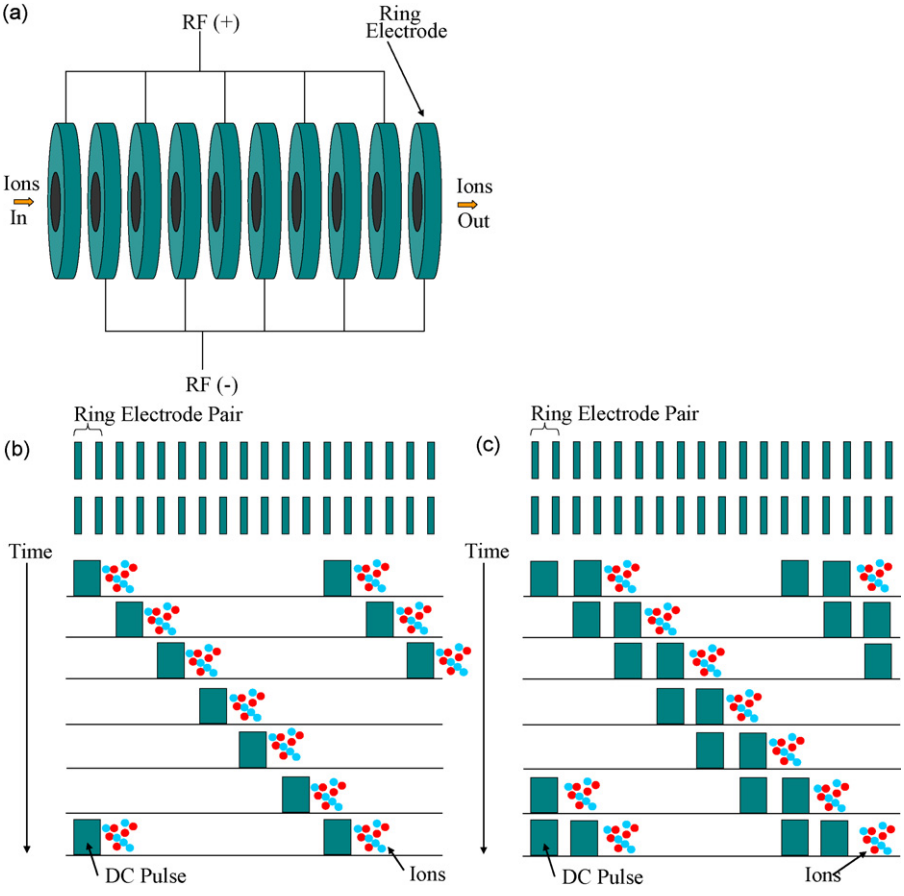

Fig. 1. (a) a schematic diagram of a stacked-ring ion guide (SRIG) (b) an illustration of the motion of the travelling wave (T-Wave) through the SRIG (c) an illustration of the motion of a two plate pair wide travelling wave in the SRIG (see Section 4.3).

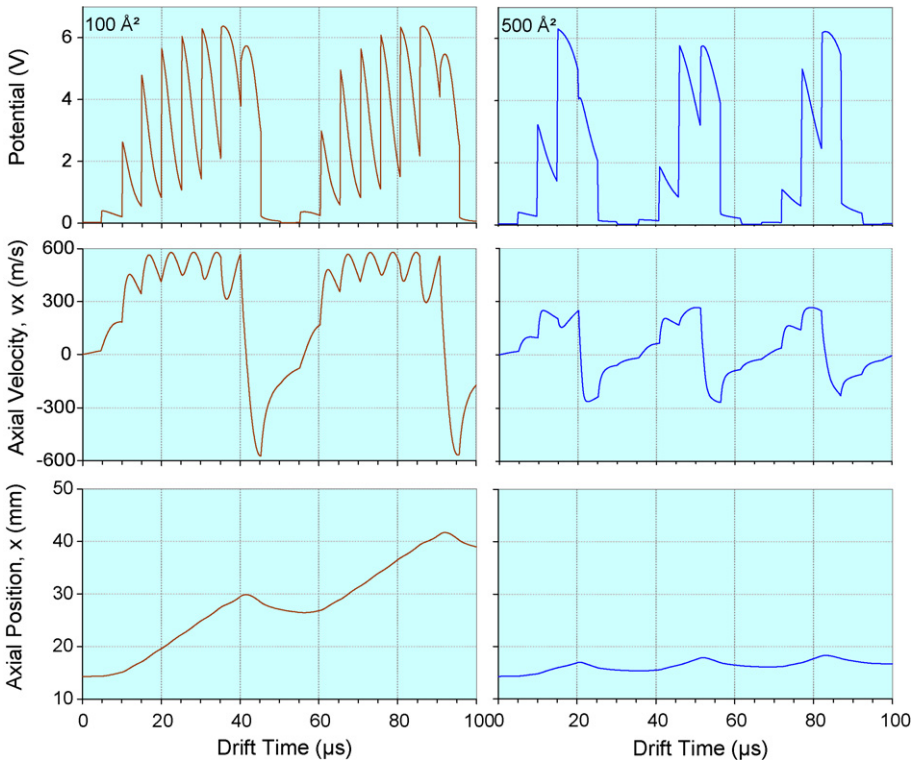

Fig. 2. Results from a SIMION simulation of T-Wave mobility separation for two ion species of the same m/z but with different CCS values. The left hand plots are for a 100 Å^2 ion and the right hand plots for a 500 Å^2 ion. The T-Wave used in the simulation was 10 V in amplitude and with a velocity of 600 m/s (≡ 5 μs pulse dwell per plate pair). The x-axis reference is the central longitudinal axis of the SRIG.

visualization of effect of the T-Wave on ion motion, ions were confined to the central longitudinal axis of the SRIG and no RF voltage was simulated on the electrodes. The data plotted in Fig. 2 are the temporal records of the ion potential, velocity and axial position in the SRIG as the travelling waves pass through. In this simulation the travelling wave pulse dwells for 5 μs on a plate pair before jumping to the next plate pair and so on, this stepwise motion results in the discrete changes to the potential and velocity of the ion species that can be seen in Fig. 2. The velocity of the higher mobility ion (smaller CCS) is, on average, higher than that of the low mobility ion as the wave approaches and so it spends more time on the wave front before being overtaken, at which point the velocity becomes negative for a period as it experiences the trailing edge of the pulse (at around 40 μs). Subsequently the next wave in the sequence approaches the ion and the process is repeated. It can be readily seen in the axial position plots of Fig. 2 that the lower mobility ion species (larger CCS) progresses more slowly through the device than the higher mobility species as the waves pass through.

Through consideration of the ion motion in the T-Wave mobility separator, it became apparent that the transition between an ion species just being carried along on a single wave through the device to just being overtaken by the wave would define a unique mobility. Furthermore, under the threshold condition where an ion species was just surfing along with a single wave, its motion on the wave front must be such that it travels a distance which is exactly that which the wave jumps in the dwell time of a pulse on each plate pair, i.e., it would perform repeat trajectories on the wave front throughout the device. Consequently, with a knowledge of the electrical potential profile of the wave in the SRIG, the electric field experienced by the ion species could be determined and used to derive a mobility value by using the adapted form of Eq. (1):

$$v(x) = KE(x) \quad (3)$$

where $v(x)$ is now the instantaneous drift velocity of the ion at point x on the wave, as produced by the electric field $E(x)$ at that point. Thus, with the determined mobility value from Eq. (3), CCS values could then be determined using Eq. (2), as for a standard drift tube.

Information on the shape of the wave in the SRIG has been obtained using SIMION modelling. The T-Wave voltage applied to a plate pair relaxes towards the central axis of the SRIG due to the effect of neighbouring plates and penetrates along the axis of the device as can be seen in Fig. 3. The electrical potential along the longitudinal (x) axis of the device approximates very well to a Gaussian form, with the peak amplitude being 0.63× that of the applied voltage. Whilst some radial distribution of the ions will occur around the longitudinal axis, the lowest potential is on axis and it is that potential which will determine the threshold between an ion species surfing and being overtaken by a wave. Consequently, a simplification is made in the subsequent calculations in that only the on-axis electrical potential profile is considered. As such, using a Gaussian profile for $E(x)$ in Eq.

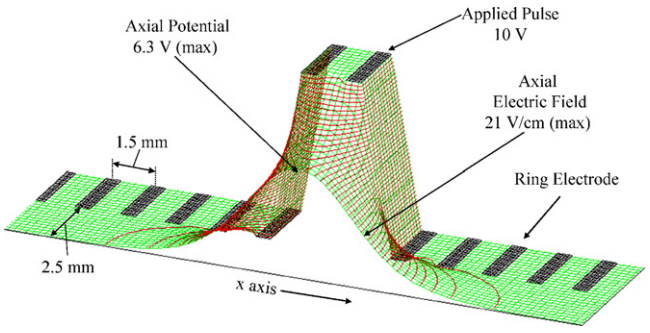

Fig. 3. A cross-section through the potential profile of a 10 V T-Wave pulse in the SRIG, generated using SIMION.

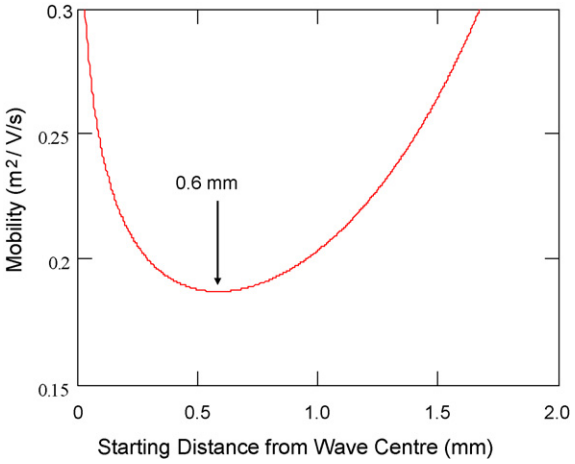

Fig. 4. A plot of the mobility of an ion species required to travel the 3 mm electrode spacing in the 10 μs (300 m/s) pulse dwell time (10 V pulse), as a function of the distance that the ion starts its motion in front of the wave centre. The minimum mobility value at 0.6 mm relates to the species that is at the threshold of being overtaken by the wave.

(3) above and rearranging for K, the following expression can be obtained,

$$K = \int_{x_0}^{x_0+s} \frac{1}{E(x)} \cdot \frac{1}{t_d} \tag{4}$$

which was then integrated numerically using Mathcad [34] to establish the mobility of an ion species that would travel the plate pair repeat distance (s = 3 mm) in the SRIG in the pulse dwell time (t_d), for different ion starting positions (x_0) on the wave front. The results of these calculations are shown in Fig. 4. As can be seen, the calculated mobility goes through a minimum value for an ion species starting approximately 0.6 mm in front of the pulse centre (at x = 0 mm) and this defines the mobility of the species that is only just keeping up with the wave. Under these conditions, the minimum mobility species would travel from 0.6 to 3.6 mm in front of the wave in the dwell time before the wave jumps the 3 mm to the next plate pair. The velocity profile of the ion species as it travels along the mobility device at this threshold condition is shown in Fig. 5. The motion is uniform and periodic, due to the fact that the electric field at the start and end points of the motion on each wave happen to be the same, i.e., there are no discontinuities in the velocity. NB although the wave does not travel in a continuous manner through the device, the concept of a travelling wave

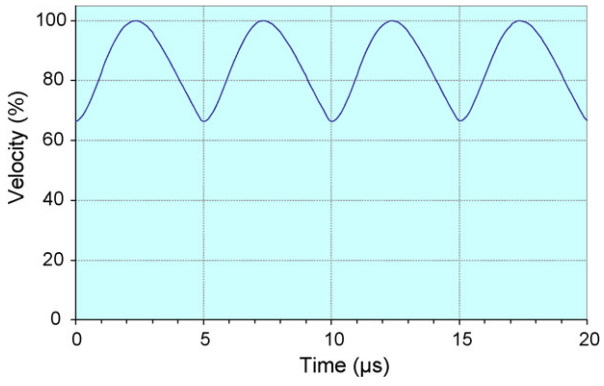

Fig. 5. Results of a SIMION simulation of the velocity of an ion species which is at the threshold of being overtaken by the wave. The simulation is for a wave with 5 μs dwell time per plate pair (≡ 600 m/s) and shows four steps of the wave through the SRIG.

'velocity' is occasionally used in the text and is defined by the ratio of the plate pair spacing to the pulse dwell time on a plate pair.

Since the Gaussian form of the pulse profile only varies in amplitude with the applied voltage, any species with the minimum mobility required to just keep up with the wave (K_{min}) will always follow the trajectory that starts 0.6 mm in front of the wave and have the exact velocity profile shown in Fig. 5. Consequently, a straightforward relationship relating K_{min} to the applied pulse voltage, V_{app}, and the pulse dwell time, t_d, can be produced from Eq. (4) by setting x_0 to 0.6 mm:

$$K_{min} = \frac{18.7}{V_{app} t_d} \tag{5}$$

where V_{app} is in volts and t_d is in microseconds. Consequently, by determining experimentally the voltage at which an ion species just starts fully surfing on a wave of known velocity, the mobility of that ion species can be determined.

The equivalent of Eq. (5) for a linear drift tube L is (from Eq. (1)),

$$K_i = \frac{L^2}{V t_i} \tag{6}$$

where K_i is the mobility of species i, t_i is the drift time of species i, L is the length of the cell and V the voltage drop across the cell. In comparison with Eq. (6), the derived constant in Eq. (5) is dependent on the Gaussian potential profile of the wave which in turn depends on the geometry of the SRIG. In determining mobility values the approaches for a drift tube experiment and the T-Wave are subtly different: in the drift tube V is fixed and the various ion drift times, t_i, are used to determine mobility values, whereas, in the T-Wave system, the drift time is fixed at t_d and V_{app} is changed to have the ion species of interest have this drift time, i.e., just keep up with the wave. Note that t_d represents the drift time on one wave front; in practice the ion repeats this trajectory 61 times on transit through the T-Wave mobility device as it comprises 61 plate pairs.

3. Experimental

All experiments were performed on a modified Synapt HDMS instrument (Waters Corp., Milford, MA, USA), the details of which have been described in a previous publication [18]. In brief, the instrument has a quadrupole/ion mobility/orthogonal acceleration time-of-flight (oa-ToF) geometry and was operated with an electrospray ionisation source in positive mode for the current work. The ion mobility section of the instrument has three T-Wave cells, the first (Trap T-Wave) is used to accumulate ions prior to gated release into the second (Mobility T-Wave) where mobility separation occurs. The third (Transfer T-Wave) transports the mobility-separated ion species to the oa-ToF for mass analysis. Ion arrival time distributions (ATDs) are obtained by synchronisation of the ToF mass spectral acquisitions with the gated release of ions into the mobility T-Wave cell. Following each gate, 200 sequential mass spectra (≡ 200 orthogonal acceleration events) are recorded, covering the millisecond mobility separation timescale. Successive blocks of 200 spectra are histogrammed for a specified acquisition time to produce the final mobility chromatogram. Instrument control and data acquisition were performed using MassLynx (v4.1) software.

To undertake the direct mobility measurements, three changes were made to the instrument: firstly, the entrance and exit apertures of the Mobility T-Wave cell were reduced to 1 mm diameter from 2 mm to allow use of higher cell pressures; secondly, the pirani gauge used to monitor the cell pressure was replaced with a capacitance manometer (Baratron 626A (0-2 Torr), MKS Ltd, Altrincham, UK) to allow accurate pressure measurement for derivation of CCS values from recorded mobilities, and thirdly, the standard T-Wave

control electronics was modified to provide more accurate control of the T-Wave pulse amplitude for determining the mobility values.

The Mobility T-Wave cell was operated at 2.5 mbar of helium and the T-Wave velocity and amplitude adjusted to allow determination of the value at which a particular ion species just started to fully surf on a single wave. The helium temperature was considered to be that of the nominal room temperature, 22 °C. The Trap and Transfer T-Wave cells were operated at approximately 5×10^{-2} mbar with approximately 20% argon and 80% helium (streaming in from the mobility cell). The Trap T-Wave was operated with a wave velocity of 300 m/s and an amplitude of 8 V. The gate was opened for 100 μs each mobility experiment to admit ions, the length of each mobility experiment depended on the *m*/*z* of the ion species being investigated, but was typically in the range of 10–15 ms. The Transfer T-Wave was operated with a wave velocity of 300 m/s and an amplitude of 5 V. The three T-Wave devices were operated with 2.7 MHz RF at 300 V pk–pk.

The samples under investigation were infused at 5 μL/min into the electrospray source of the Synapt and the *m*/*z* of the ion species of interest selected using the quadrupole prior to mobility analysis.

The following samples were used in this study: equine myoglobin, equine cytochrome c, bovine ubiquitin, gramicidin S, leucine enkephalin, substance P, bradykinin, obtained from Sigma–Aldrich (Poole, UK) and a yeast enolase digest (Waters Mass Prep. Digestion Standard, Waters, Milford, MA). These samples were chosen based on the availability of drift tube derived CCS data for comparison purposes. Each of the samples was dissolved in a 50:50 water:methanol solution acidified with 0.1% formic acid to give solution strengths around the pmol/μL level.

4. Results and discussion

4.1. Leucine enkephalin (leu-enk) study

The main focus of the experimental investigation is to establish as accurately as possible the pulse voltage at which an ion species just starts to surf on a single wave.

Leu-enk was infused into the system and the $[M+H]^+$ ion at *m*/*z* 556 selected for mobility analysis. The ATD for *m*/*z* 556 was recorded at various pulse voltages and the resultant data are shown in Fig. 6. The wave velocity used was 300 m/s which equates to a 10 μs pulse dwell time per electrode pair.

There are two distinct regions on the plot in Fig. 6. Firstly, at pulses above about 14 V the ions are being transported through the mobility cell on a single wave and the arrival time remains constant. At pulses below about 12.8 V all the ions are undergoing mobility separation by the waves periodically overtaking them and the arrival time increases with decreasing pulse voltage. The pulse voltage at which all of the *m*/*z* 556 ions just begin to surf on a single wave occurs at around 13.8 V. It is evident from the plot that some of the ions surf through the system on a single wave from as low as 13 V, on the leading edge of the ATD. However, since the potential on axis is the lowest point of the pulse radial potential profile, it is there that the last population of ions will still be overtaken by the wave if the pulse amplitude is not high enough, and so will represent the threshold value between all ions surfing, or not.

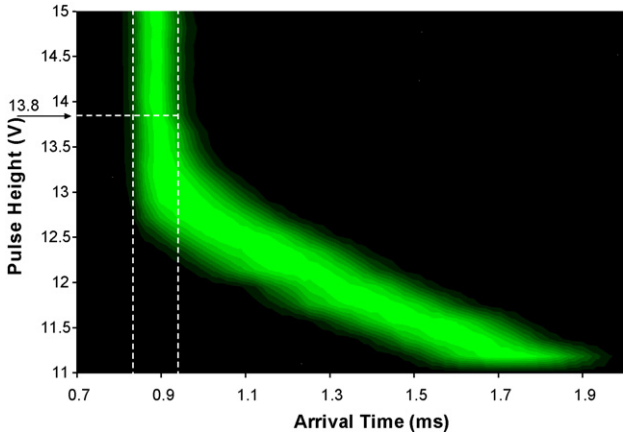

Fig. 6. A heat map plot of the arrival time of the *m*/*z* 556 ion of leu-enk in the T-Wave mobility cell as a function of applied pulse amplitude. The two dashed vertical lines illustrate where the ion species surf completely on a single wave. The pulse amplitude of 13.8 V is the threshold where all ions surf on a single wave.

Using the 13.8 V pulse amplitude and the 10 μs pulse dwell time, from Eq. (4) a mobility of 0.136 m^2/V/s is determined for the *m*/*z* 556 ion of leu-enk. Thus with the helium at 2.5 mbar and nominally 22 °C, a CCS value of 161 $Å^2$ is calculated from Eq. (2), this is in excellent agreement with the 162 $Å^2$ reported in a previous drift tube study [35].

A consideration with this approach for determining mobility values is whether the experimental conditions are such that the electric field driven motion of the ions through the gas does not raise the energy of the ion species beyond thermal energies, the so-called low field limit. At values higher than this limit, the mobility of an ion species is no longer independent of the electric field strength. The relevant term used to define this low field limit is the ratio of the electric field, *E*, to the neutral gas number density, *N*. The requirement for operating in the low field limit is given by the semi-quantitative expression [20,21]:

$$\frac{E}{N} < \left[\frac{m_i}{m_i + m_n}\right]^{1/2} \frac{d^2}{z} \tag{7}$$

where *E*/*N* is in units of Townsends (1 Td = 10^{-17} Vcm^2), and *d* is the diameter of the ion in Å. Using the approximation that $\Omega \approx \pi d^2$ [20], Eq. (7) gives a value of 51 Td for the low field limit for leu-enk. From the present study, the highest electric field experienced by the leu-enk on the wave front is 28 V/cm which equates to an *E*/*N* of 43 Td which is within the low field limit and so indicates that the CCS value obtained from this approach is valid.

In consideration of the low field limit it is worth noting that on the axis of the SRIG, the fields experienced by the ion from the confining RF are small in comparison with those from the pulse voltage and so can be ignored. Moving radially off axis in the device, the penetration of the RF is more significant and could potentially cause some heating of the ions, however, to date no effects of this type have been identified in the T-Wave mobility device. Further, the CCS data presented here indicates that use of RF ion confinement is not a major issue in this device, either in terms of ion heating or in the measurement of CCS values, at least for the ion species investigated.

4.2. Singly charged ion species

To further evaluate the capability of this direct T-Wave mobility measurement approach, the same procedure as above was used to investigate the singly charged $[M+H]^+$ ions of gramicidin S (*m*/*z* 1142), bradykinin (*m*/*z* 1061), substance P (*m*/*z* 1348) and the GVFR peptide (*m*/*z* 478) from a digest of yeast enolase.

The results are shown in Table 1, together with the literature values for the CCSs determined using drift tube systems. As can be seen there is once again very good agreement between the T-Wave derived CCS values and those obtained using drift tubes, with all systems falling below the low field limit.

Table 1
Experimental data on CCS values obtained for some singly charged ion species using the direct T-Wave mobility method together with the drift tube derived literature values. NB a pulse dwell time of 15 μs (≡200 m/s) was used for all data except leu-enk which was 10 μs (≡300 m/s).

	m/z	*z*	Pulse amplitude	T-Wave mobility	T-Wave *E/N* (max)	Low field limit *E/N*	T-Wave CCS	Literature value	Error
			V	$m^2/V/s$	Td	Td	$Å^2$	$Å^2$ [Ref.]	%
Leu-enk	556	1	13.8	0.136	43	51	161	162 [35]	−0.6
Substance P	1348	1	16.2	0.077	50	93	284	292 [36]	−2.7
Gramicidin S	1142	1	14.7	0.085	46	84	257	263 [36]	−2.3
Bradykinin	1061	1	13.3	0.094	41	78	233	245 [36]	−4.9
GVFR	478	1	12.5	0.150	39	47	146	147 [37]	−0.7

Table 2
Experimental data on CCS values obtained for the multiply charged ions of equine myoglobin, equine cytochrome c and bovine ubiquitin using the direct T-Wave mobility method together with the drift tube derived literature values. A pulse dwell time of 15 μs (≡200 m/s) was used for all data.

	m/z	*z*	Pulse amplitude	T-Wave mobility	T-Wave *E/N* (max)	Low field limit *E/N*	T-Wave CCS	Literature value	Error
			V	$m^2/V/s$	Td	Td	$Å^2$	$Å^2$ [Ref. [38]]	%
Myoglobin	1305	13	13.4	0.093	42	77	3053	3136	−2.6
Myoglobin	772	22	10.4	0.120	32	55	4004	3815	5.0
Ubiquitin	1225	7	12.3	0.101	38	72	1514	1580	−4.2
Ubiquitin	778	11	9.7	0.129	30	52	1862	1802	3.3
Cytochrome c	1124	11	11.7	0.107	36	67	2246	2303	−2.5
Cytochrome c	687	18	8.9	0.140	28	49	2808	2766	1.5

Table 3
Experimental data on CCS values obtained for the multiply charged ions of equine myoglobin using the direct T-Wave mobility method together with the drift tube derived literature values. In this case, pulses were applied to two plate pairs at a time but progressing only one plate pair per pulse dwell time. A pulse dwell time of 15 μs (≡200 m/s) was used for all data.

m/z	*z*	Pulse amplitude	T-Wave mobility	T-Wave *E/N* (max)	Low field limit *E/N*	T-Wave CCS	Literature value	Error
		V	$m^2/V/s$	Td	Td	$Å^2$	$Å^2$ [Ref. [38]]	%
772	22	7.9	0.125	29	55	3835	3815	0.5
808	21	8.0	0.123	29	57	3723	3792	−1.8
849	20	8.2	0.12	30	59	3646	3682	−1.0
893	19	8.4	0.117	30	60	3542	3570	−0.8
943	18	8.6	0.115	31	62	3420	3489	−2.0
998	17	9.0	0.110	33	63	3396	3384	0.4
1060	16	9.3	0.106	34	66	3281	3313	−1.0
1131	15	9.5	0.104	34	69	3171	3230	−1.8
1212	14	10.0	0.099	36	71	3098	3143	−1.4
1305	13	10.5	0.094	38	77	3027	3136	−3.5
1414	12	11.0	0.090	40	81	2918	3044	−4.1
1542	11	11.7	0.084	42	85	2847	2942	−3.2

4.3. Multiply charged ion species

At this point, the species investigated have all been singly charged. To establish whether the approach would be of utility for multiply charged species, various proteins were investigated. The samples of equine myoglobin (Mw 16,951), equine cytochrome c (Mw 12,359) and bovine ubiquitin (Mw 8,565) were infused separately into the electrospray source of the Synapt and the various charge state species selected using the quadrupole for mobility analysis. The results of this study are given in Table 2 where again there is very good agreement with the CCS data obtained using drift tubes [38], illustrating that this direct T-Wave measurement approach is also valid for larger, multiply charged species. Once again, all of the experiments conducted were within the low field limit.

As part of these studies, other T-Wave pulse patterns were investigated. One of particular interest was the use of a two plate pair wide pulse instead of one, but with the pulse step remaining at one plate pair (see Fig. 1(c)). The benefit of this from an operational point is that the on-axis potential in the SRIG increases from 0.63× the applied voltage to 0.9×, thus extending the effective range of the electronics. Using the same theoretical approach as described earlier, the axial pulse profile was modelled using two superimposed Gaussian distributions, and this used to determine mobilities in the same way using Eq. (3). To investigate the use of this pulse pattern for determining mobilities, the sample of equine myoglobin was re-run and the charge state species ranging from +22 to +11 (*m/z* 772 to 1542) were analysed. The data are presented in Table 3 along with the drift tube derived CCS values from Ref. [38]. It can be seen that there is excellent agreement between the T-Wave derived CCS values and those obtained using drift tubes, also, there is good agreement with the values obtained using the single plate pair pulse in Table 2. As expected, the pulse amplitude thresholds are lower than those determined in the previous study.

Whilst the direct T-Wave approach is relatively straightforward for determining the mobilities of those multiply charged protein species where only a single mobility peak is present (i.e., one or similar CCS conformations), it is somewhat more problematic for the cases where multiple peaks are observed. If the ATDs are reasonably well separated then the pulse voltage at which the more mobile species begins to fully surf can be established before the ions from the lower mobility species begin to surf on the wave. If the peaks are not well separated then it is difficult to determine the threshold point shown in Fig. 6 for the more mobile species due to interference from the lower mobility species. However, the mobility of the lowest mobility species can always be determined.

5. Conclusions

Whilst ion mobility spectrometry as a technique has been investigated for many years, the last 10 or so have seen a growth in interest for analytical and biological applications. In recent years, the availability of a commercial IM-MS instrument in the Synapt has given many more analysts and researchers access to investigate possible uses of ion mobility separation in their field of study. A particular area of interest has been in the determination of collision cross-section data to allow inferences in structures of gas phase ions. Whilst the T-Wave mobility separation device in the Synapt instrument has not been as directly amenable to such measurements as, for instance a drift tube system, an ever-increasing number of studies indicate that calibration of the mobility separation is possible.

The studies presented here describe an alternative mode of operation of the T-Wave mobility separator to allow direct determination of ion mobility values, and subsequently collision cross-section data. This approach has been shown to provide collision cross-section data which are within 5% or so of those values obtained using drift tube systems. Further work to improve the accuracy of this method will include a more rigorous means of determining the threshold pulse voltages from the data and more detailed investigation into the effect of operational parameters of the T-Wave mobility cell on the calculated mobilities.

References

[1] G.A. Eiceman, Z. Karpas, Ion Mobility Spectrometry, see, for example, second ed., CRC Press, Boca Raton, 2005.
[2] T. Wyttenbach, M.T. Bowers, Top. Curr. Chem. 225 (2003) 207.
[3] J.A. McLean, B.T. Ruotolo, K.J. Gillig, D.H. Russell, Int. J. Mass Spectrom. 240 (2005) 301.
[4] A.B. Kanu, P. Dwivedi, M. Tam, L. Matz, H.H. Hill, J. Mass Spectrom. 43 (2008) 1.
[5] B.C. Bohrer, S.I. Merenbloom, S.L. Koeniger, A.E. Hildebrand, D.E. Clemmer, Annu. Rev. Anal. Chem. 1 (2008) 293.
[6] K.J. Gillig, B.T. Ruotolo, E.G. Stone, D.H. Russell, Int. J. Mass Spectrom. 239 (2004) 43.
[7] G. Javahery, B. Thomson, J. Am. Soc. Mass Spectrom. 8 (1997) 697.
[8] K. Thalassinos, S. Slade, K.R. Jennings, J.H. Scrivens, K. Giles, J. Wildgoose, J. Hoyes, R.H. Bateman, M.T. Bowers, Int. J. Mass Spectrom. 236 (2004) 55.
[9] Y. Guo, J. Wang, G. Javahery, B.A. Thomson, K.W.M. Siu, Anal. Chem. 77 (2005) 266.
[10] K. Tang, A.A. Shvartsburg, H.N. Lee, D.C. Prior, M.A. Buschbach, F. Li, A.V. Tolmachev, G.A. Anderson, R.D. Smith, Anal. Chem. 77 (2005) 3330.
[11] S.I. Merenbloom, S.L. Koeniger, S.J. Valentine, M.D. Plasencia, D.E. Clemmer, Anal. Chem. 78 (2006) 2802.
[12] C.S. Hoaglund, S.J. Valentine, D.E. Clemmer, Anal. Chem. 69 (1997) 4156.
[13] T. Wyttenbach, P.R. Kemper, M.T. Bowers, Int. J. Mass Spectrom. 212 (2001) 13.
[14] S. Myung, Y.J. Lee, M.H. Moon, J. Taraszka, R. Sowell, S. Koeniger, A.E. Hilderbrand, S.J. Valentine, L. Cherbas, P. Cherbas, T.C. Kaufmann, D.F. Miller, Y. Mechref, M.V. Novotny, M.A. Ewing, C.R. Sporleder, D.E. Clemmer, Anal. Chem. 75 (2003) 5137.
[15] G. von Helden, T. Wyttenbach, M.T. Bowers, Int. J. Mass Spectrom. Ion Proc. 146/147 (1995) 349.
[16] D.E. Clemmer, M.F. Jarrold, J. Mass Spectrom. 32 (1997) 577.
[17] K.J. Gillig, B. Ruotolo, E.G. Stone, D.H. Russell, K. Fuhrer, M. Gonin, A.J. Schultz, Anal. Chem. 72 (2000) 3965.
[18] S.D. Pringle, K. Giles, J.L. Wildgoose, J.P. Williams, S.E. Slade, R.H. Bateman, M.T. Bowers, J.H. Scrivens, Int. J. Mass Spectrom. 261 (2007) 1.
[19] K. Giles, S.D. Pringle, K.R. Worthington, D. Little, J.L. Wildgoose, R.H. Bateman, Rapid Commun. Mass Spectrom. 18 (2004) 2401.
[20] H.E. Revercomb, E.A. Mason, Anal. Chem. 47 (1975) 970.
[21] E.A. Mason, E.W. McDaniel, Transport Properties of Ions in Gases, Wiley, New York, 1988.
[22] A.A. Shvartsburg, R.D. Smith, Anal. Chem. 80 (2008) 9689.
[23] B.T. Ruotolo, K. Giles, I. Campuzano, A.M. Sandercock, R.H. Bateman, C.V. Robinson, Science 310 (2005) 1658.
[24] J.L. Wildgoose, K. Giles, S.D. Pringle, S. Koeniger, S. Valentine, R.H. Bateman, D.E. Clemmer, ASMS Proceedings, Seattle, 2006.
[25] J.H. Scrivens, K. Thalassinos, G.R. Hilton, S.E. Slade, T.J.T. Pinherio, R.H. Bateman, M. Grabenauer, M.T. Bowers, ASMS Proceedings, Indianapolis, 2007.
[26] K. Giles, J.L. Wildgoose, D.L. Langridge, ASMS Proceedings, Denver, 2008.
[27] B.T. Ruotolo, J.L. Benesch, A.M. Sandercock, S.J. Hyung, C.V. Robinson, Nat. Protoc. 3 (2008) 1139.
[28] J.P. Williams, J.H. Scrivens, Rapid Commun. Mass Spectrom. 22 (2008) 187.
[29] K. Thalassinos, M. Grabenauer, S.E. Slade, G.R. Hilton, M.T. Bowers, J.H. Scrivens, Anal. Chem. 81 (2009) 248.
[30] D.P. Smith, T.W. Knapman, I. Campuzano, R.W. Malham, J.T. Berryman, S.E. Radford, A.E. Ashcroft, Eur. J. Mass Spectrom. 15 (2009) 113.
[31] J.P. Williams, T. Bugarcic, A. Habtemariam, K. Giles, I. Campuzano, P.M. Rodger, P.J. Sadler, J. Am. Soc. Mass Spectrom. 20 (2009) 1119.
[32] SIMION Version 8, SIS Inc., Ringoes, NJ.
[33] C.M. Lock, E.W. Dyer, Rapid Commun. Mass Spectrom. 13 (1999) 422.
[34] Mathcad version 13, Mathsoft, Parametric Technology Corp., Needham, MA.
[35] N.C. Polfer, B.C. Bohrer, M.D. Plasencia, B. Paizs, D.E. Clemmer, J. Phys. Chem. A 112 (2008) 1286.
[36] B.T. Ruotolo, C.C. Tate, D.H. Russell, J. Am. Soc. Mass Spectrom. 15 (2004) 870.
[37] S.J. Valentine, A.E. Counterman, D.E. Clemmer, J. Am. Soc. Mass Spectrom. 10 (1999) 1188.
[38] www.indiana.edu/∼clemmer/.